Printed in U.S.A.

an ASME publication

$1.00 PER COPY
50¢ TO ASME MEMBERS

Thermal-Stress and Low-Cycle Fatigue Data on Typical Materials

K. E. HORTON

Senior Metallurgist, Advanced Technology Laboratories Division of American-Standard, Mountain View, Calif.

J. M. HALLANDER

Assistant Metallurgist, Advanced Technology Laboratories Division of American-Standard, Mountain View, Calif.

D. D. FOLEY

Northrop Aircraft, Newbury Park, Calif.

This paper presents the results of low-cycle-fatigue tests wherein either thermal strain or mechanical strain was the independent variable. The materials investigated were primarily ferrous alloys for use in nuclear reactors. The analysis of results was based on plastic-strain-range measurements which could be made reproducibly in the 2×10^{-5} range. Graphs of plastic strain range versus cycles to failure were often found to be independent of large variations in temperature and cycle time. The results from thermal-fatigue and constant-temperature-fatigue tests were usually indistinguishable on these graphs, suggesting that identical metallurgical phenomena occurred in each type of test.

THE AMERICAN SOCIETY OF MECHANICAL ENGINEERS, UNITED ENGINEERING CENTER, 345 EAST 47th STREET, NEW YORK, N.Y. 10017

Thermal-Stress and Low-Cycle Fatigue Data on Typical Materials

K. E. HORTON

D. D. FOLEY

J. M. HALLANDER

The creation of cyclic thermal stresses by cyclic temperature variations has long been recognized as a possible source of fatigue fracture. Prominent among the many occurrences of cyclic temperature variations are those found in the components of power-generating equipment, such as turbines and nuclear reactors. Since the thermal-fatigue conditions in such equipment are generally of low-frequency occurrence, the problem is one of low-cycle fatigue failure.

Analysis of the problem is complicated because temperature and stress are both variable in thermal fatigue. The typical analysis, in terms of stress range versus cycles to failure for conventional constant-temperature fatigue is found to be almost totally unacceptable, often giving graphs resembling shotgun patterns. With stress unsuitable as a basis for analysis, it is necessary to use strain; and since elastic strain is nondamaging, it is desirable to use plastic strain.

Previous studies of thermal fatigue based on plastic-strain analysis yielded interesting results that usually did not coincide with known, conventional-fatigue data, even when both types of fatigue tests were made under nearly identical conditions. While these inconsistencies have largely been eliminated in recent studies, they have more or less required that conventional-fatigue studies be performed whenever thermal-fatigue studies are done in order to insure meaningful results and interpretation thereof.

TEST SPECIMENS AND APPARATUS

The test-specimen design used in this study is considered a standard thermal-fatigue (TF) specimen, as it has been widely used since 1953. The specimen is shown in Fig.1, together with the maximum temperature gradient existing along the gage length. The position and length of the measurement gage length, ℓ_o',[1] are seen to prevent a significant thermal gradient from existing within the ℓ_o'. The lack of a thermal gradient within ℓ_o' signifies the lack of a strain gradient also, which is of course an extremely desirable situation in TF studies.

The test specimen is placed in a fixture and firmly gripped at the shoulders such that neither expansion nor contraction can occur; however,

since the specimen is connected in series with a 10,000-lb load cell, some movement is allowed. Cyclic thermal stresses are caused by alternately passing an electric current through the specimen until the desired maximum temperature of cycling is reached (T_2) and cooling the specimen by flowing air through the axial hole until the minimum temperature of cycling is reached (T_1). The test fixture, specimen, and extensometer are shown in operation in Fig.2. The extensometer contains a differential transformer to detect movement and weighs less than 1 oz completely assembled. It is clamped on the specimen with a spring force of less than 2 ounces.

Temperature is controlled and measured with 28-gage chromel/alumel thermocouple wires spot-welded on the specimen within the ℓ_o'. A very small welding current is used to attach the thermocouples in an effort to minimize the influence of the thermocouple on the specimen. The rate of temperature change is controlled to give a strain rate (unconstrained) of 0.0005 in/in-sec.

In addition to the recordings of temperature, load, and ℓ_o' movement required to ascertain strain (as explained in the next section), continuous recordings of load and temperature are made on all test machines. The recording of load versus time is used to determine failure, since a fatigue crack would cause an abrupt decrease in cyclic tensile load. In the latter stages of the test program, a novel relay mechanism was devised and attached to the load recorder such that a drop in load would cause the test machine to shut down. Prior to this, automatic shutdown was accomplished by temperature monitoring. In both cases, automatic shutdown invariably signaled that a crack at least 1/8 in. in length had penetrated through the specimen wall.

The composition and as-received condition of the materials studied in this program are listed in Table 1. Because all stock for any given alloy was from one heat, the composition of test specimens was considered constant.

---

[1] The length of ℓ_o' is determined by the distance between extensometer arms.
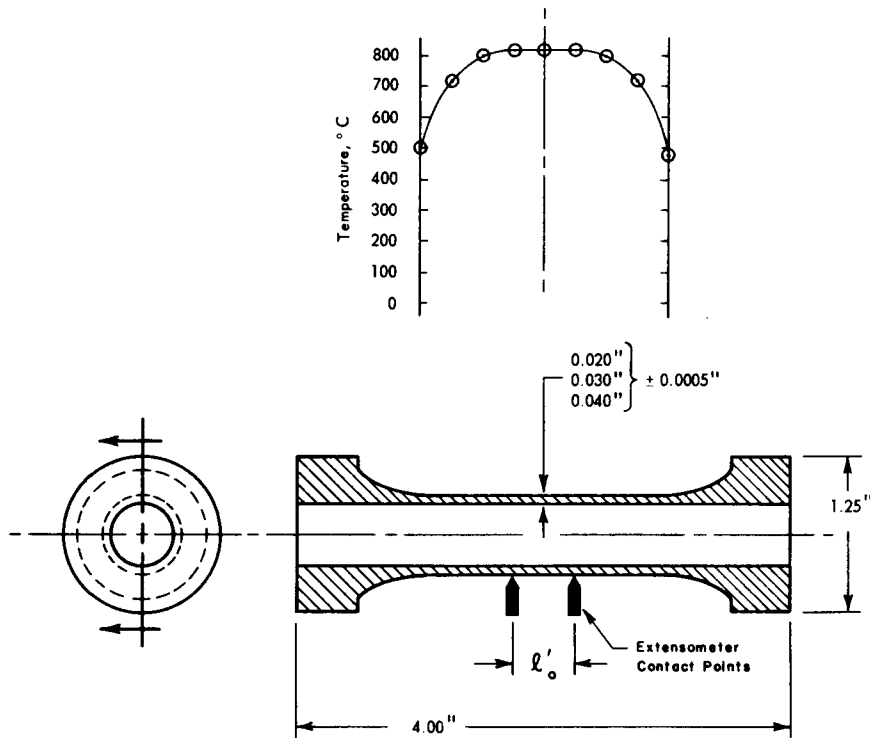
Fig. 1 TF and CF specimen and temperature gradient at end of heating cycle
(with no hold time at temperature extremes)
heating rate = 30 deg C/sec
finish = 16 μ in. or better

STRAIN MEASUREMENT

When a constrained specimen is thermally cycled, the equation describing the movement of the extensometer arms is

$$\ell_o' \left[\frac{\sigma_4 - \sigma_3}{E} + \epsilon_p + a(T_4 - T_3) \right] = \ell_{o,4}' - \ell_{o,3}' \quad (1)$$

where the subscripts represent different points in

NOMENCLATURE

C = material constant (related to ductility $N^{k'} \Delta\epsilon_p = C$)(dimensionless)

E = modulus of elasticity, psi

k = material constant ($\sigma = k\epsilon_p^n$)(dimensionless)

k' = material constant ($N^{k'} \Delta\epsilon_p = C$) (dimensionless)

ℓ_o' = measurement gage length (length over which strain readings are taken), in.

M = proportionality constant $= \left[N(\Delta W)/(M\Delta\epsilon_p)^m \right]$

m = slope of $N(\Delta W)$ versus $N(\Delta\epsilon_p)$ curve

N = cycles to failure

N_i = particular cycle number

n = strain-hardening exponent

P = load, lb

T = temperature

T_m = mean temperature of cycling = $(T_2 - T_1)/2$

T_1 = lowest temperature of cycling

T_2 = highest temperature of cycling

T_3 = temperature at which zero stress occurs

on heating

T_4 = temperature at which zero stress occurs on cooling

t = specimen wall thickness, in.

ΔW = plastic strain energy per cycle (from area of stress-strain hysteresis loop), in-lb/in.^{3}

Y = width of hysteresis loop

Z = correction to movement equation, equation (1)

a = coefficient of thermal expansion (averaged over $T_2 - T_1$), in./in.-deg C

ϵ_p = plastic strain, in/in

$\Delta\epsilon$ = strain range, in/in

1st subscript	2nd subscript
e = elastic	i = measurement at any given cycle
p = plastic	
t = total	

σ = stress, psi

$\Delta\sigma_m$ = maximum stress range (tension plus compression) per cycle at half life, psi

3

TABLE 1   COMPOSITION OF TEST PROGRAM ALLOYS (Wt pct Except as Noted)

Alloy	As-received Condition	C	Mn	Si	P	S	Cr	Ni	Cu	Mo	Co	Fe	Sn	Hf	N_2	O_2	Zr	Ti	Al	B
304-L Stainless Steel	Cold-worked (18% RA)†	0.018	1.32	0.65	0.009	0.011	18.22	10.51	0.30	0.25		Bal.								
304 Stainless Steel	Annealed	0.05	0.88	0.50	0.028	0.011	18.71	9.84				Bal.								
403 Stainless Steel	Annealed	0.10	0.51	0.30	0.008	0.009	12.47	0.34				Bal.								
A302-B Steel	Normalized	0.22	1.3	0.20	0.040	0.040				0.5		Bal.								
A387-D Steel (Croloy 2-1/4)	Annealed	0.10	0.48	0.36	0.014	0.017	2.24			0.94		Bal.								
Incoloy 800	Annealed	0.06	1.08	0.64	0.004	0.006	20.9	32.9	0.02		0.025	Bal								
Zircaloy-2	Cold-worked (27% RA)†	0.024*		0.003*			0.07*	0.06*				0.128*	1.41	0.0045	0.0055*	0.12*	Bal.			
Rene 41‡	Solution-treated	0.08	0.10	0.25		0.0005	19.4	Bal.		9.19	11.91	0.74						3.12	1.40	0.0042

* Atomic percent.
† RA = reduction in area.
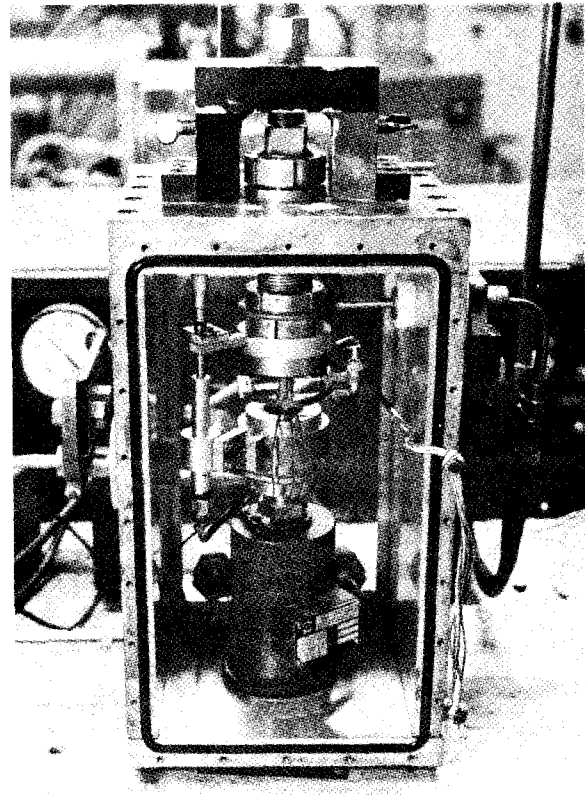‡ Supplied by General Electric Metallurgical Products Department.

Fig. 2 TF test machine shown with specimen, extenso-
meters, and load cell in place (vacuum-tight front
cover removed)

a cycle. In the TF tests performed in this and most other studies, thermal strain $[a(T_4 - T_3)]$ is the independent variable; hence it would seem desirable to measure mechanical strain versus cycles to failure. Carrying the strain-measurement argument one step further would lead to the measurement of cyclic plastic strain since only plastic strain causes failure.

It was mentioned previously that thermal strain was the independent variable in these tests and thus it was not possible to control the plastic strain range, $\Delta\epsilon_p$, such that it could be held constant during a test. However, it has been found that, after the first few cycles of a test, $\Delta\epsilon_p$ becomes constant and the total actual plastic strain

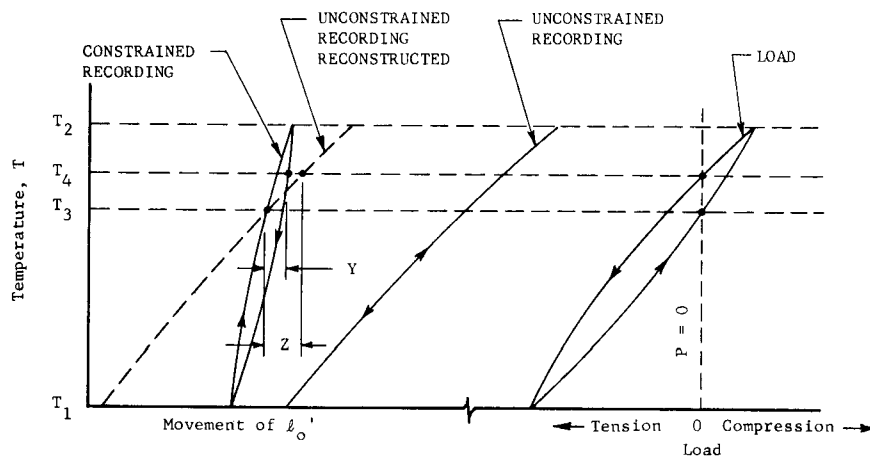$$2\sum_{i=1}^{N} N_i \, \Delta\epsilon_{p,i} \qquad (2)$$

is essentially the same as

$$2N\Delta\epsilon_p \qquad (3)$$

when $\Delta\epsilon_p$ is measured at half-life. However, if such metallurgical changes as annealing occur dur-

4
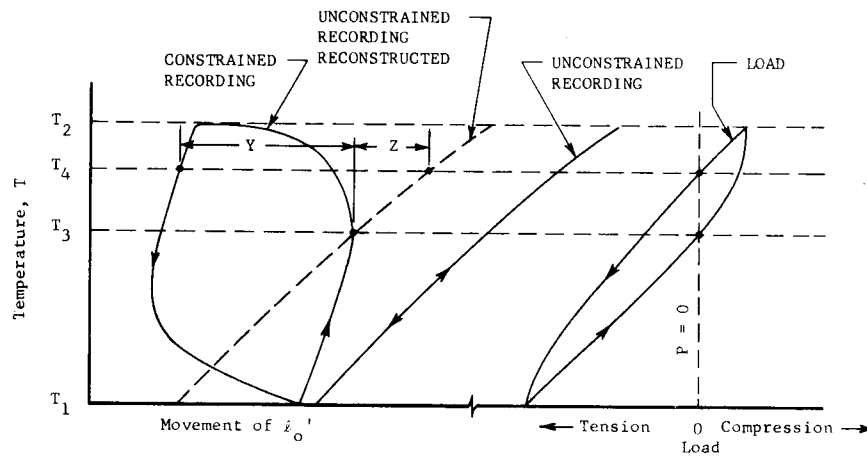
a. $\ell_o{}'$ Under More than 100% Constraint, $\Delta\epsilon_p = \dfrac{Y + Z}{\ell_o{}'}$

b. $\ell_o{}'$ Under Less than 100% Constraint, $\Delta\epsilon_p = \dfrac{Z - Y}{\ell_o{}'}$

Fig. 3 Graphical method of obtaining plastic strain range, $\Delta\epsilon_p$

ing a fatigue test, $\Delta\epsilon_{p,i}$ may vary continuously during the test so that equation (3) will not be a valid substitute for equation (2). This situation is manifested by the relatively large number of strain measurements made during each fatigue test. On graphs using $\Delta\epsilon_p$, the average value for the test is used.

There are various methods of extracting plastic strain from equation (1). The method found best in this study was to select points 3 and 4 as the zero-load points of a cycle, with equation (1) becoming

$$\ell_o{}'\left[\Delta\epsilon_p + a(T_4 - T_3)\right] = \Delta\ell_o{}' \qquad (4)$$

The technique described subsequently was then used to obtain $\Delta\epsilon_p$. This technique is entirely graphical and does not require knowledge of the coeffi-

cient of thermal expansion. All that need be known is $\ell_o{}'$.

The technique of measuring $\Delta\epsilon_p$ is illustrated in Fig. 3 for two different constraint conditions. An X-Y recorder is used to record unconstrained $\ell_o{}'$ movement versus temperature, constrained $\ell_o{}'$ movement versus temperature, and load versus temperature. The width (Y) of the hysteresis loop for constrained movement versus temperature at zero-load points $(\Delta\ell_o{}')$ is of course an indication of the plastic strain that has occurred during one half-cycle, but since the zero-load points occur at different temperatures a correction must be made to the loop width. The correction, for an $\ell_o{}'$ under more than 100 percent constraint, is
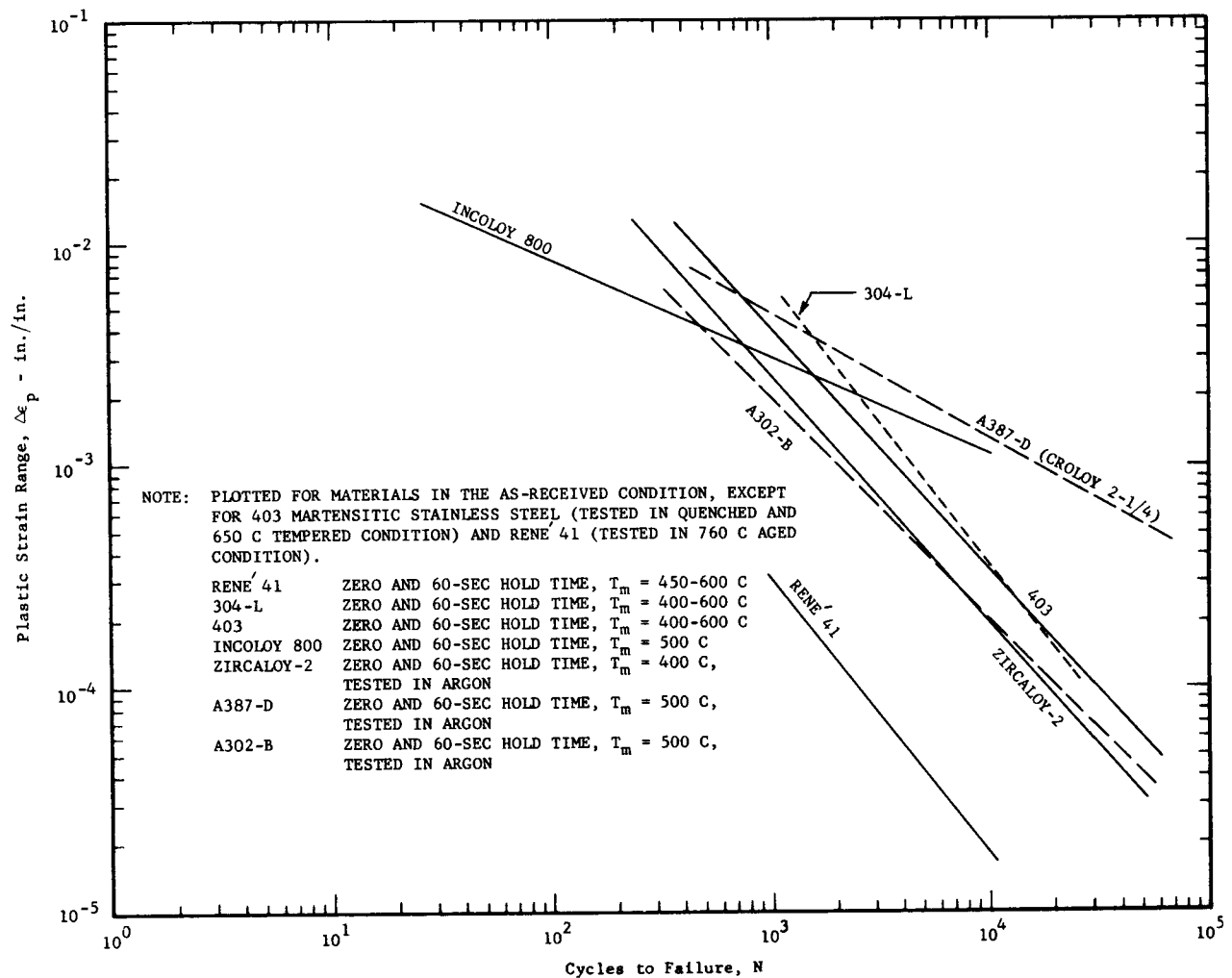
$$Z = a (T_4 - T_3) \ell_o{}' \qquad (5)$$

5

Fig. 4 Summary of TF results on alloys tested in this program $\Delta \epsilon_p$ versus N [tested in air, unless otherwise noted. See reference (6) for details]

and is determined graphically by superimposing the unconstrained recording on the constrained recording as shown in Fig. 3. If ℓ_0' is under less than 100 percent constraint, i.e., ℓ_0' is physically longer at T_4 than at T_3 and $T_4 > T_3$, the correction is reversed. The foregoing technique gave reproducible results at values of $\Delta \epsilon_p$ = 0.00002 in./in.

TESTING PROCEDURE

The equipment available throughout most of the TF test program used thermal strain as the independent variable. Consequently, when a specimen was at the highest temperature of the cycle it was in compression, while at the lowest temperature it was in tension. This situation existed regardless of whether the specimen was initially clamped at the lowest or the highest temperature (T_1 and T_2, respectively) of the cycle. After the specimen

had cycled for 10 percent of its estimated life, X-Y recordings were made of load versus temperature and ℓ_0' movement versus temperature. The specimen was then unclamped and an X-Y recording of ℓ_0' movement versus temperature was taken, followed by reclamping at the average temperature of zero load and continued thermal cycling. The reclamping operation has been found to have no effect on the fatigue life of the specimen. X-Y recordings were thereafter made at every 20 percent of expected life and/or once a day. The schedule of data acquisition insured that X-Y recordings were available at specimen half life.

TEST RESULTS AND DISCUSSION

The TF test results are summarized in Figs. 4 and 5 for, respectively, plastic-strain range versus cycles to failure, N, and stress range versus

6

NOTE: PLOTTED FOR MATERIALS IN THE AS-RECEIVED CONDITION, EXCEPT
FOR 403 MARTENSITIC STAINLESS STEEL (TESTED IN QUENCHED AND
650 C TEMPERED CONDITION) AND RENE 41 (TESTED IN 760 C AGED
CONDITION).

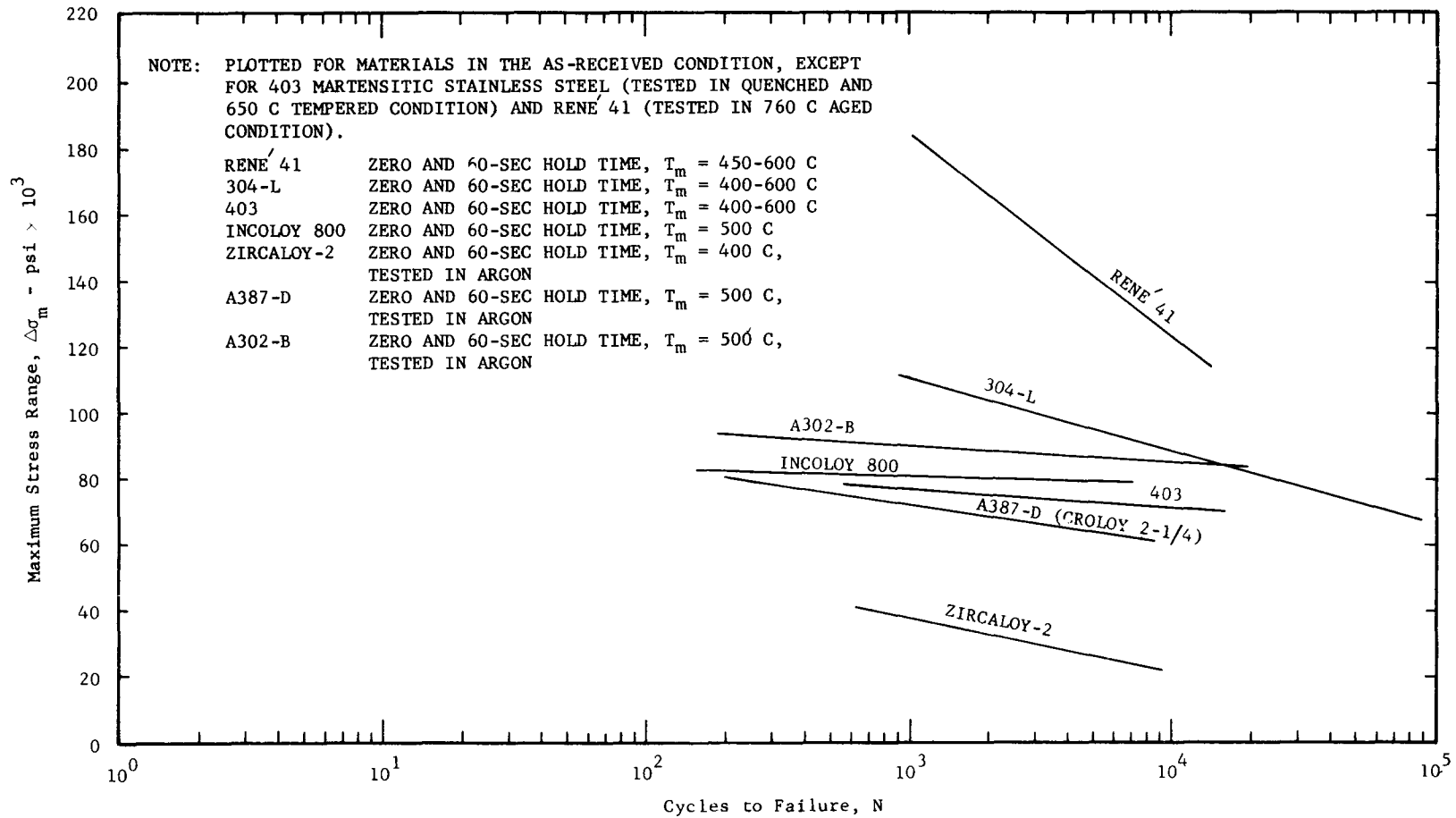|	
RENE 41	ZERO AND 60-SEC HOLD TIME, T_m = 450-600 C
304-L	ZERO AND 60-SEC HOLD TIME, T_m = 400-600 C
403	ZERO AND 60-SEC HOLD TIME, T_m = 400-600 C
INCOLOY 800	ZERO AND 60-SEC HOLD TIME, T_m = 500 C
ZIRCALOY-2	ZERO AND 60-SEC HOLD TIME, T_m = 400 C, TESTED IN ARGON
A387-D	ZERO AND 60-SEC HOLD TIME, T_m = 500 C, TESTED IN ARGON
A302-B	ZERO AND 60-SEC HOLD TIME, T_m = 500 C, TESTED IN ARGON

Fig.5   Summary of TF results on alloys tested in this program $\Delta \sigma_m$ versus N (tested in air, unless otherwise noted)
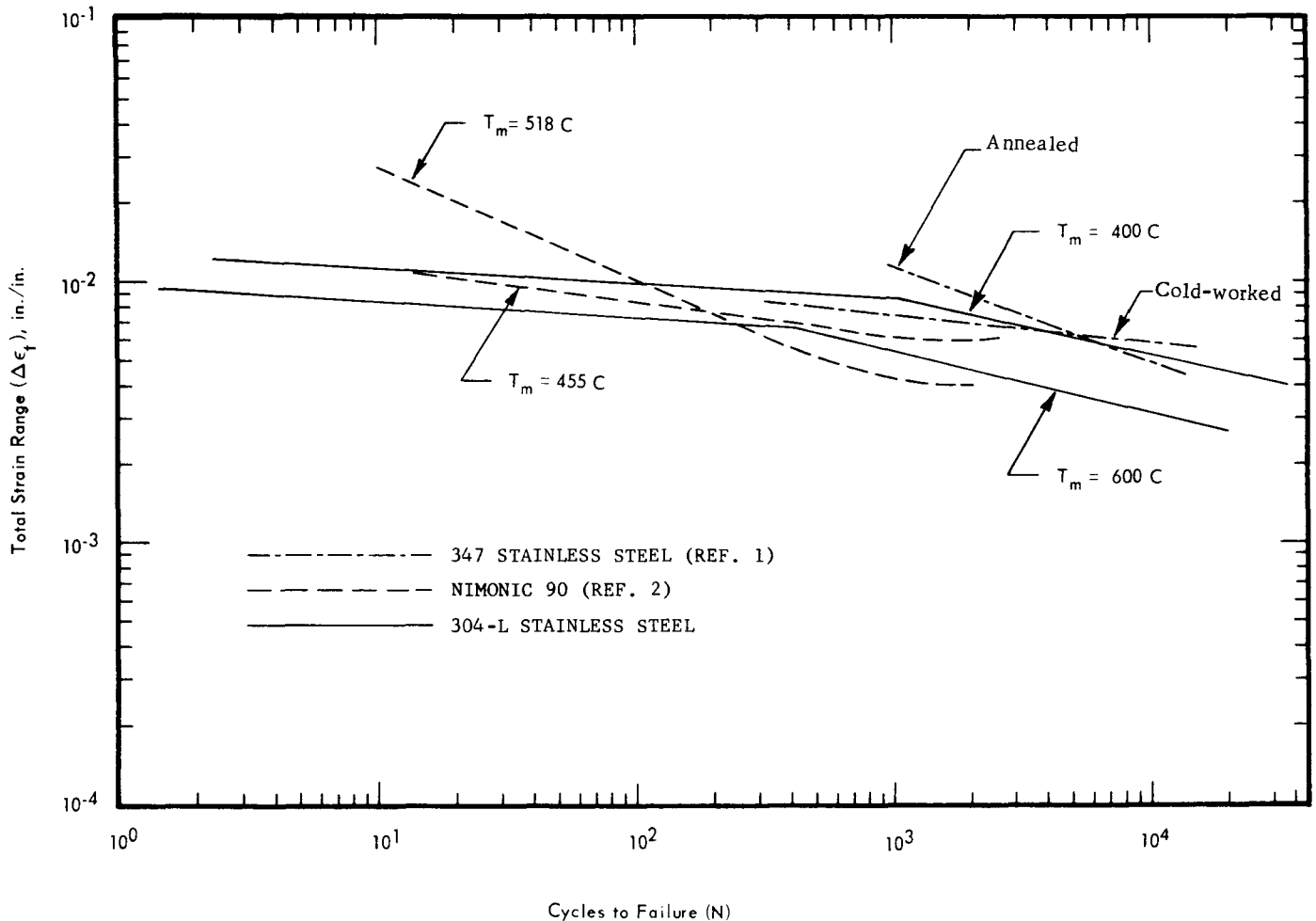
Fig. 6 TF data for annealed 304-L stainless steel and Nimonic 90 $\Delta\epsilon_t$ versus N

N. These curves indicate that some alloys, such as Zircaloy-2, are consistently inferior on both bases of comparison (but not over all N-ranges). Other alloys, such as 304-L stainless steel, are superior on both bases of comparison over certain ranges of $\Delta\epsilon_p$ and then become inferior outside these ranges. The behavior of René 41 (tested after aging 16 hr at 760 C) falls between the two aforementioned tendencies.

In order for an alloy to be consistently superior or inferior on both a stress and a plastic-strain basis of comparison, it would appear that a comparison of toughness (as measured, for example, by the area under a tensile-test, stress-strain curve) would confirm the relative fatigue resistance. A cross plot of Figs. 4 and 5 confirms this theory. The difference in philosophy in using Figs. 4 and 5 is clearly that in the former one would choose an alloy for superior TF resistance by calculating the expected (required) $\Delta\epsilon_p$, whereas the latter figure would be consulted after first calculating the expected (required) $\Delta\sigma_m$.

Just as the superiority of one material over another in TF was shown to depend frequently on the range of fatigue, the superiority of one material condition over another possible condition has also been shown to be a function of stress or strain range. Coffin ([1])[2] has found that annealed 347 stainless steel is superior in TF to cold-worked 347 in the low N-range (high $\Delta\epsilon_p$ and $\Delta\sigma_m$-range), whereas cold-worked 347 is superior to annealed 347 in the high N-range, Fig. 6. These results were explained by considering dislocation density and cyclic stresses; that is, in the high $\Delta\sigma_m$-range, a cold-worked, high-dislocation-density material would have a greater lattice disorder than the annealed material; dislocation cycling would thus cause fatigue cracks to form sooner in the cold-worked material condition. On the other hand, the cold-worked material condition is superior in the low $\Delta\sigma_m$-range because dislocation motion would be less and a fatigue crack would not form as soon as it would in the annealed material condition.

_____

[2] Underlined numbers in parentheses designate References at the end of the paper.
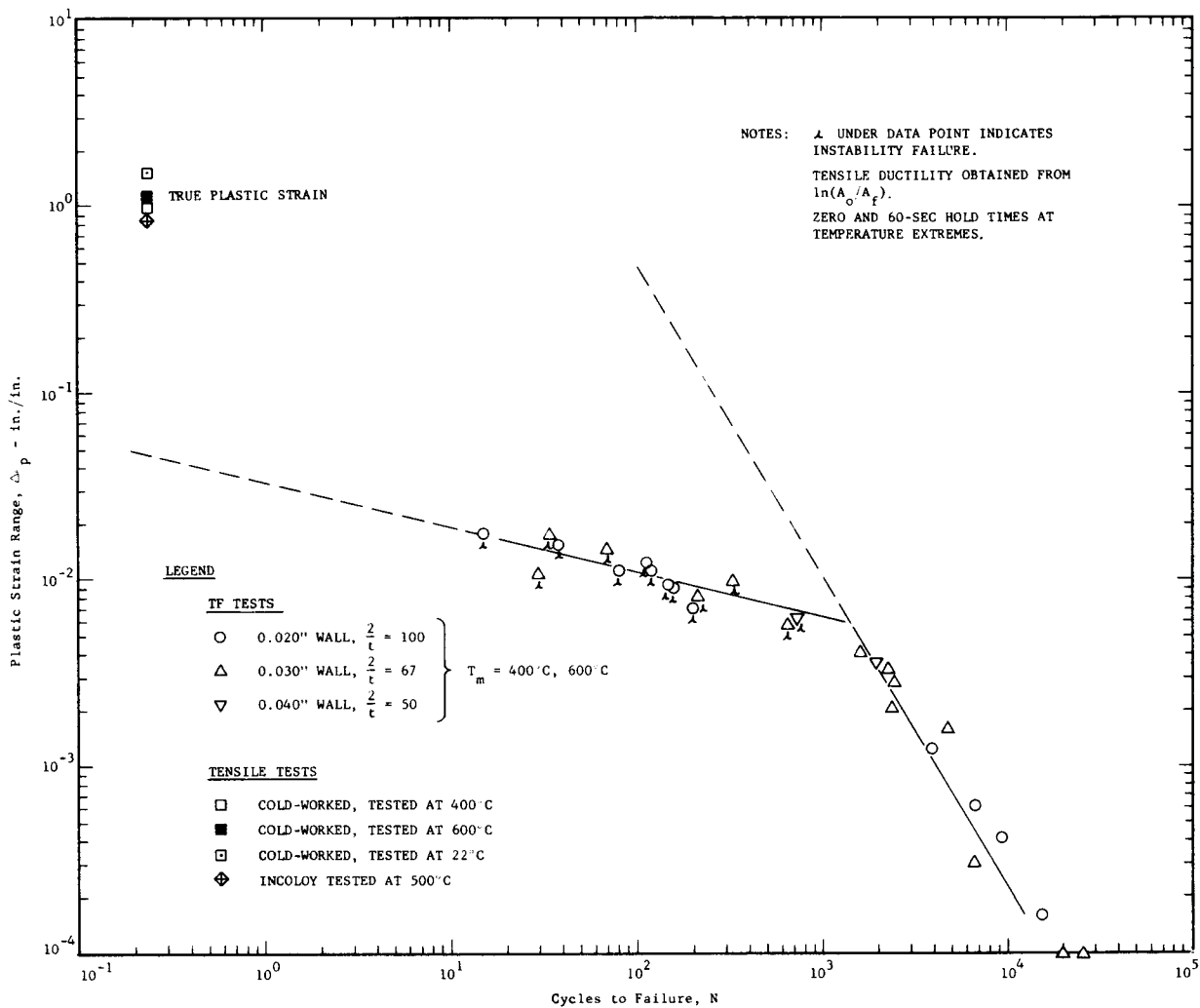
8

Fig. 7 TF and tensile-test data for cold-worked 304-L austenitic stainless steel $\Delta\epsilon_p$ versus N

A similar argument for the superiority of the high-strength condition over the low-strength condition in TF has been advanced for a nickel-base, Nimonic 90 alloy (2) (see also Fig.6). Instead of comparing the cold-worked with the annealed condition, the author compared high T_m tests (low-strength condition) with low T_m tests (high-strength condition) and observed that in the high $\Delta\epsilon_p$-range (where $\Delta\epsilon_p \cong \Delta\epsilon_t$), the more ductile high T_m tests showed results superior to the less ductile low T_m tests. The reverse was true in the high N-range where elastic strain range $\Delta\epsilon_e \rightarrow$ total strain range, $\Delta\epsilon_t$. These results were explained by considering the material to be more ductile at high T_m and therefore more capable of withstanding the $\Delta\epsilon_p$ in a region (low N) where $\Delta\epsilon_p$ predominates over $\Delta\epsilon_e$. Conversely, in the high N-range, the material tested at low T_m is stronger and more resistant to $\Delta\epsilon_e$ in a range where $\Delta\epsilon_e$ of course far exceeds $\Delta\epsilon_p$.

In both of the foregoing arguments, the comparison is based on a required cyclic strain in the low N-region but a required cyclic stress in the high N-region, even though strain is the independent variable. The fallacy in the arguments is seen when one considers, for example, a required cyclic strain in the high N-range. For a fixed $\Delta\epsilon_t$, the cold-worked material would be cycling through a greater $\Delta\sigma_m$ than the annealed material and the ability to withstand $\Delta\epsilon_p$ would be the life-limiting factor. Similarly, fixed $\Delta\epsilon_t$ tests in the high N-range would result in a greater $\Delta\sigma_m$ for the low T_m tests than for the high T_m tests and superior TF resistance would again belong to the situation in which the material had the greatest ability to withstand the resulting $\Delta\epsilon_p$.

Some of the results of the foregoing investigations are plotted in Fig.6 along with test results on cold-worked 304-L stainless steel. The low T_m tests on 304-L are superior to the high T_m
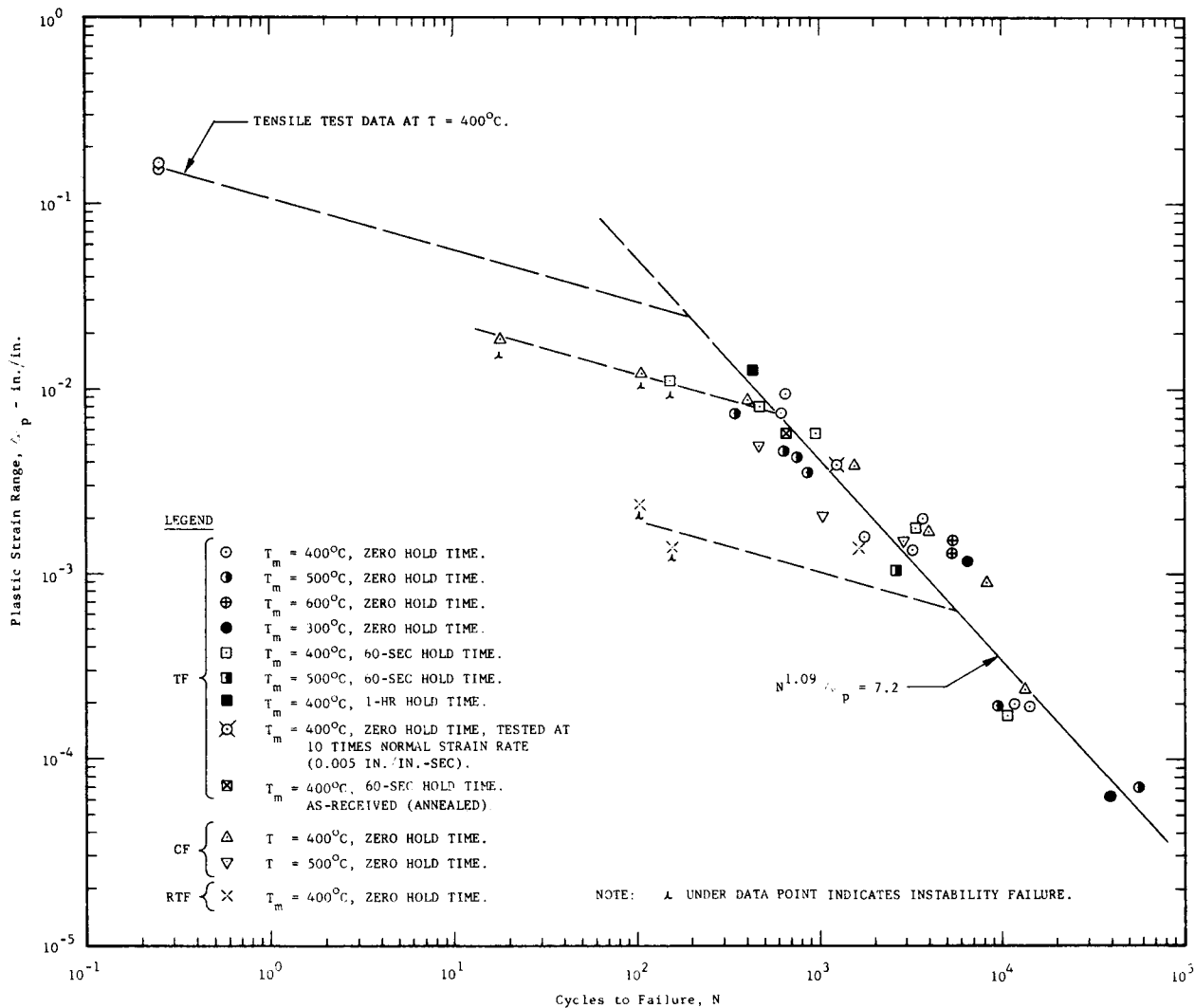
9

Fig. 8 Fatigue-test results for 403 Martensitic stainless steel (tested after quench and tempering to Rockwell hardness C-20) $\Delta\epsilon_p$ versus N

tests in all N-ranges, indicating that the material has a greater ability to withstand $\Delta\epsilon_p$ when TF cycling at low T_m. Tensile tests on cold-worked 304-L reveal that this alloy has greater ductility at the low temperature, thus substantiating the greater ability of this material to withstand $\Delta\epsilon_p$ at the lower T_m.

The inherent ability of a material to withstand cyclic plastic strain is equal to

$$2N\Delta\epsilon_p \qquad (6)$$

and it has been found that this quantity is proportional to N to some power. For example, the relation

$$2N\Delta\epsilon_p = C\ N^{1/2} \qquad (7)$$

was obtained by Coffin (1). Equation (7) can

easily be transformed to an equation of the type

$$N^{k'}\Delta\epsilon_p = C \qquad (8)$$

where the quantity on the left might logically be termed the modified ability to withstand plastic strain. Ideally, this quantity is constant for a material for all fatigue-test conditions; in actuality, it is often found to vary, as does even k'. To illustrate, the equation for TF failure of 403 martensitic stainless steel is

$$N^{1.09}\Delta\epsilon_p = 7.2 \qquad (9)$$

and it is not changed by varying T_m between 400 and 600 C or by varying the hold time at temperature extremes between zero and 60 sec. It is noteworthy that this same equation is also valid

10

for constant-temperature, push-pull fatigue tests at 400 and 600 C.[3]

On the other hand, the TF failure equation for annealed 304-L stainless steel is

$$N^{0.14}\Delta\epsilon_p = 1.2 \qquad (10)$$

at $T_m = 400$ C, but at $T_m = 600$ C, it becomes

$$N^{0.24}\Delta\epsilon_p = 1.4 \qquad (11)$$

Similarly, the TF failure equation for annealed 304-L is different from the equation for cold-worked 304-L, the annealed material being superior over all values of N. However, the fatigue-failure equation for 304-L stainless steel (both cold-worked and annealed) was found to be relatively independent of hold time at temperature extremes, grain size, mean temperature (except as noted in the foregoing), and the means of applying strain (i.e., whether TF or CF).

Equivalence of TF and CF

The equivalence of TF and CF (mechanical-strain independent) is to be expected whenever identical metallurgical phenomena occur during fatigue. Such agreement of these two types of test results was unfortunately not obtained until recently. Perhaps the major cause for failure to obtain agreement between TF and CF tests in the past was the measurement of an average strain that was significantly less than the maximum strain occurring in the TF test due to a temperature gradient inside the measurement gage length. Such a thermal gradient did not usually exist in CF tests, since the specimens were not heated by the Joule method.

It would of course be possible to get equivalent TF and CF results by changing the CF test conditions until agreement resulted. However, the equivalence mentioned in the foregoing was obtained under similar TF and CF test conditions. For example, identical strain rates and hold times at cycle extremes were used in TF and CF tests, and CF tests were performed in the temperature range near the mean temperature of thermal cycling in TF tests.

The equivalence of TF and CF tests has also been obtained elsewhere, notably by Carden (3) on a Hastelloy alloy. Conversely, Taira (4) did not get equivalence on stainless steels, probably because of the thermal gradient present in his TF tests.

Instable Failure

The method of TF testing used in this pro-

3

These tests are designated here as conventional-fatigue tests (CF).

gram, that of thermal cycling a tubular specimen, often leads to buckling, i.e., instable failure, and premature failure. The presence of buckling is manifested in the failure graphs by the appearance of two distinct lines. For example, TF testing of cold-worked 304-L austenitic stainless-steel specimens of varying wall thickness led to the graph shown in Fig.7 (5). Clearly, specimen wall thickness does not affect the geometric stability of the specimen. However, it is possible that a specimen-volume effect was counteracting a change-in-stability effect in these tests. It is further noticed that tensile test results obtained under conditions similar to those existing in TF tests did not agree with either the pure-fatigue (no buckling) or the instable-fatigue (buckled) results. The tensile-test specimens exhibited necking down in the fracture region. This necking is considered representative of an instable material condition, but this instability is of lesser magnitude than the gross buckling of instable-fatigue failures.

Test results (6) for a quenched and tempered 403 martensitic stainless steel are shown, in Fig. 8, to substantiate the results discussed in the foregoing for 304-L austenitic stainless steel. Again it is noticed that two failure lines exist for stable and instable failures and that tensile-test data do not agree with either fatigue-failure line. To test a hypothesis of degrees of instability, some reverse thermal fatigue (RTF) tests were performed on this steel. These RTF tests put the specimen in tension at the higher temperatures of the cycle and in compression at the lower temperatures. It was thought (incorrectly) that these tests would permit the specimen to undergo very large $\Delta\epsilon_p$ without buckling. In actuality, however, it was found that the specimens were more instable in RTF; that is, very large compressive loads were built up near T_1 such that column buckling occurred early in fatigue. Nevertheless, the hypothesis was believed to be verified; i.e., varying degrees of instability cause a series of instable-fatigue-failure lines, with the apparently least instable of the instable failures being the specimens subjected to tensile testing.

When RTF tests were performed in the lower $\Delta\epsilon_p$ range such that pure-fatigue failures occurred, the results agreed with the TF and CF test results. This observation has been recorded elsewhere (7).

Energy to Failure

The relatively low-cycle fatigue investigated in this study permitted the measurement of cyclic plastic strain, whereas in high-cycle fatigue (over 10^6 cycles) this measurement is usually not possible. Plastic strain obviously occurs in
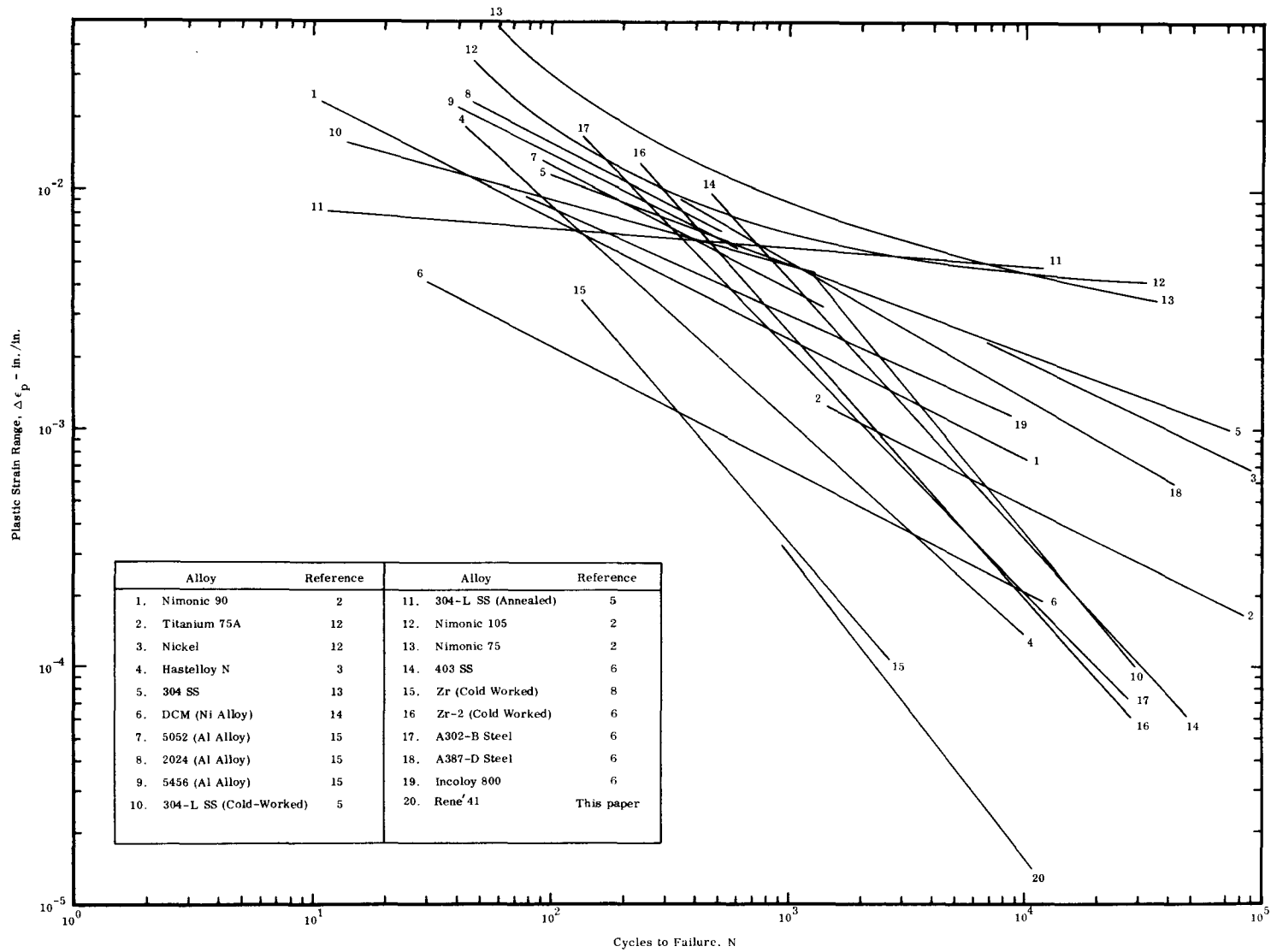
11

Fig. 9   Summary of all pertinent TF data in technical literature $\Delta\varepsilon_p$ versus N

	Alloy	Reference		Alloy	Reference
1.	Nimonic 90	2	11.	304-L SS (Annealed)	5
2.	Titanium 75A	12	12.	Nimonic 105	2
3.	Nickel	12	13.	Nimonic 75	2
4.	Hastelloy N	3	14.	403 SS	6
5.	304 SS	13	15.	Zr (Cold Worked)	8
6.	DCM (Ni Alloy)	14	16.	Zr-2 (Cold Worked)	6
7.	5052 (Al Alloy)	15	17.	A302-B Steel	6
8.	2024 (Al Alloy)	15	18.	A387-D Steel	6
9.	5456 (Al Alloy)	15	19.	Incoloy 800	6
10.	304-L SS (Cold-Worked)	5	20.	Rene 41	This paper

high-cycle fatigue, but it is essentially a micro-scopic phenomenon that is localized at certain points in the specimen, which eventually may form fatigue cracks. It is therefore impossible to measure absorbed strain energy in high-cycle fa-tigue, and this quantity is important since it is a measure of damage to the specimen. Conversely, absorbed strain energy can be measured in low-cycle fatigue, and these measurements provide in-teresting conclusions as discussed next.

TF tests on zirconium (8) indicated that the total plastic strain to failure increased with in-creasing fatigue life (decreasing $\Delta\epsilon_p$), and it is feasible to predict that total absorbed strain en-ergy would also follow this trend. Such a trend was indeed observed for 304-L (9) and 403 stainless steels and for Croloy $2^1/4$ steel (6) cycled in TF. One of the equations describing this trend is

$$N\Delta W = 1.3 \times 10^3 N^{0.64} \qquad (12)$$

Morrow's data (10) indicate that the corresponding equation for 4340 steel would be (for CF tests)

$$N\Delta W = 1.4 \times 10^5 N^{0.35} \qquad (13)$$

If an idealized hysteresis loop is assumed such that

$$\Delta W = 2 \int_0^{\Delta\epsilon_p} \sigma d\epsilon_p \qquad (14)$$

it is possible to derive a quasi-theoretical fa-tigue-failure equation utilizing the total-energy-to-failure equations mentioned previously. For example, it is empirically known (6) that

$$N\Delta W = M(N\Delta\epsilon_p)^m = 6 \times 10^4 (N\Delta\epsilon_p)^{1.08} \qquad (15)$$

and thus it is possible to write

$$N\Delta W = M(N\Delta\epsilon_p)^m = 2N \int_0^{\Delta\epsilon_p} \sigma d\epsilon_p \qquad (16)$$

Furthermore, it is empirically known from both tensile tests and individual hysteresis loops for TF and CF tests that

$$\sigma = k\epsilon_p^n \qquad (17)$$

Substituting equation (17) into (16) and integrat-ing results in the following equation:

$$N^{\frac{m-1}{m-n-1}} \Delta\epsilon_p = \left[\frac{2k}{M(n+1)}\right]^{\frac{1}{m-n-1}} \qquad (18)$$

Substituting the values of M and m from fatigue

tests and n and k from tensile tests for cold-worked 304-L austenitic stainless steel into equa-tion (18) gives

$$N^{2.58} \Delta\epsilon_p = 0.97 \qquad (19)$$

as compared to the purely experimentally determined equation of

$$N^{1.29} \Delta\epsilon_p = 43 \qquad (20)$$

Using values of k and n obtained from hysteresis loops did not improve the agreement between equa-tions (19) and (20). Results of similar opera-tions on the 403 martensitic stainless steel gave

$$N^{0.97} \Delta\epsilon_p = 5.4 \qquad (21)$$

theoretically and

$$N^{1.09} \Delta\epsilon_p = 7.2 \qquad (9)$$

experimentally. It is apparent that the results of this attempt to relate quasi-theoretical and empirical results left much to be desired. Simi-lar attempts on purely theoretical grounds (11) have enabled accurate prediction of the slope of the CF failure equation, (18).

Compilation of TF Results

Since the early 1950's numerous TF studies have been conducted. Coffin (1), Majors (12), and others were the pioneers of this type of test, and they deserve credit for recognizing many of the problems and manifestations of TF testing. A com-pilation of the data generated by the foregoing authors and all others in the field is shown in Fig.9. Not all the data generated by the quoted authors was used, and some investigations of TF in which strain was not measured could not be com-piled on the graph.

The slopes of the lines in Fig.9 vary con-siderably. For this reason, it is believed that a "universal" slope does not exist for TF or CF, although a slope of approximately one half is often observed. Since many of the lines on this graph are dependent on test conditions, the figure is intended only to show the general trend of TF data.

CONCLUSIONS

Thermal-fatigue and conventional-fatigue tests were performed on a variety of modern alloys. All tests were unidirectional, push-pull type on tubular specimens. The following conclusions were evident from this research:

13

1 In fatigue tests, where thermal strain is the independent variable, curves of plastic strain range, $\Delta\epsilon_p$, versus cycles to failure, N, are often independent of significant changes in test variables, such as mean temperature and hold time, and of metallurgical variables, such as grain size.

2 The ability of a material to withstand plastic strain determines its fatigue life in strain-independent tests.

3 The slopes of the failure equations as derived from curves of $\Delta\epsilon_p$ versus N vary from 0.1 to over 1.0. The often noted slope of one half for TF tests performed earlier is suggested to be a result of instable failures in the low N-range.

4 Conventional fatigue tests performed under conditions roughly approximate to those existing in TF tests often exhibit failure equations identical to TF-failure equations on graphs of $\Delta\epsilon_p$ versus N. Conversely, tensile testing under the foregoing conditions gives results that do not agree with TF-results.

5 The superior fatigue resistance of a particular alloy condition exists over all failure ranges. In no instance does an inferior material condition become superior after a change in the failure range, although such occurrences have been found on other materials. However, alloys exhibiting superior fatigue resistance in one failure range often become inferior to other alloys in a different failure range.

6 The strongest material condition, as ascertained in a tensile test, can also be the superior fatigue-resistant condition on a $\Delta\sigma_m$ versus N graph (with $\Delta\epsilon$ as the independent variable) if the ability to withstand cyclic plastic strain is nearly identical in all material conditions. Conversely, it should be possible for a weaker material condition to have superior fatigue resistance to a stronger material condition on a graph of $\Delta\sigma_m$ versus N when the ability to withstand cyclic plastic strain is significantly greater in the weaker material condition. This latter statement has not been borne out by experimentation, however.

7 The total absorbed strain energy to failure is proportional to the cycles to failure. Although it was not possible to predict accurately the fatigue-failure equation from energy considerations, it is believed that such predictions are possible.

8 The presentation of fatigue data on plastic-strain graphs permits the formulation of many plots that are independent of test variables. Such graphs cannot be obtained for high-cycle fatigue because plastic-strain range is too small to measure ($< 10^{-5}$ in/in).

9 None of the $\Delta\epsilon_p$ versus N-graphs indicated an endurance limit; however, $\Delta\epsilon_p$ versus N-graphs do not preclude the existence of an endurance limit. In the ferrous alloys studied in this program, cycling at strains less than the endurance limit $\Delta\epsilon_p$ would have required a $\Delta\epsilon_p$ smaller than could be measured.

REFERENCES

1 "A Study of the Effects of Cyclic Thermal Stresses on a Ductile Metal," by L. F. Coffin, Jr., Trans. ASME, vol. 76, August, 1954, pp. 931-950.

2 "The Thermal Fatigue Resistance of Nickel-Chromium Alloys," by P. G. Forrest and K. B. Armstrong, Paper presented at Joint International Conference on Creep, Institute of Mechanical Engineers, London, 1963.

3 "Thermal Fatigue, Part I - An Analysis of the Conventional Experimental Method," by A. E. Carden, Proceedings of the American Society for Testing Materials, vol. 63, 1963, pp. 736-758.

4 "Thermal Fatigue and Cyclic Mechanical Strain at Elevated Temperature of 18-8 Cb Stainless Steel and 2.25 Cr-1 Mo Steel," by S. Taira et al, Bulletin of the Japanese Society of Mechanical Engineers, vol. 6, no. 22, 1963, pp. 169-185.

5 "Investigation of Thermal-Stress-Fatigue Behavior of Stainless Steels, Summary of Test Results on Types 304 and 304-L Stainless Steels," by K. E. Horton, Advanced Technology Laboratories, a Division of American-Standard, ATL-A-141, EURAEC-1034, Topical Report for the U. S. Atomic Energy Commission, Joint U. S.-Euratom Research and Development Board, under Contract No. AT(04-3)-250, Project Agreement No. 11, 10 April 1964.

6 "Investigation of Thermal-Stress-Fatigue Behavior of Stainless Steels," by K. E. Horton and J. M. Hallander, American Radiator & Standard Sanitary Corporation, Advanced Technology Laboratories Division, ATL-A-144, Final Report for the U. S. Atomic Energy Commission, Joint U. S.-Euratom Research and Development Board, under Contract No. AT(04-3)-250, Project Agreement No. 11, 31 October 1964.

7 "An Investigation of Thermal-Stress Fatigue as Related to High-Temperature Piping Flexibility," by L. F. Coffin, Jr., Trans. ASME, vol. 79, 1957, pp. 1637-1651.

8 "Thermal-Stress-Fatigue Behavior of Zir-

conium and Zirconium Alloys," by K. E. Horton and R. S. Stewart, Advanced Technology Laboratories, a Division of American-Standard, ATL-A-127, Final Report for the U. S. Atomic Energy Commission under Contract No. AT(04-3)-250, Project Agreement No. 6, 31 October 1961.

9 "Thermal-Stress-Fatigue Behavior of Stainless Steels," Advanced Technology Laboratories, a Division of American-Standard, Monthly Letter Report ATL-D-976 to the U. S. Atomic Energy Commission under Contract No. AT(04-3)-250, Project Agreement No. 11, 4 February 1963.

10 "Cyclic Plastic Strain Energy and Fatigue of Metals," by J. Morrow, Paper presented at 1964 Annual Conference of the American Society of Testing Materials, Chicago, Illinois.

11 "An Investigation of Plastic Strain Energy as a Criterion for Fatigue Life," by J. Morrow, Report to the Garrett Corporation, August, 1960.

12 "Thermal and Mechanical Fatigue of Nickel and Titanium," by H. Majors, Jr., Transactions of the American Society for Metals, vol. 51, 1959, pp. 421-437.

13 "The Failure of 304 Stainless Steel by Thermal Strain Cycling at Elevated Temperature," by A. E. Carden and J. H. Sodergren, ASME Paper No. 61-WA-200, 1961.

14 "Low-Cycle Fatigue of Two Nickel-Base Alloys by Thermal-Stress Cycling," by F. J. Mehringer and R. P. Felgar, Trans. ASME, Series D, September, 1960, pp. 661-672.

15 "The Effects of Thermal Cycling Between Cryogenic and Elevated Temperatures on the Mechanical Properties of Materials," by E. B. Wiley, C. Hoggatt, and R. Venuti, University of Denver, Denver Research Institute, March, 1961.